0026-895X/06/7001-249–258$20.00
MOLECULAR PHARMACOLOGY
Copyright © 2006 The American Society for Pharmacology and Experimental Therapeutics
Mol Pharmacol 70:249–258, 2006

Vol. 70, No. 1
18804/3119475
Printed in U.S.A.

Soluble Mimics of the Cytoplasmic Face of the Human V1-Vascular Vasopressin Receptor Bind Arrestin2 and Calmodulin

Nan Wu, Rosemarie Macion-Dazard, Stanley Nithianantham, Zhen Xu,[1] Susan M. Hanson, Sergey A. Vishnivetskiy, Vsevolod V. Gurevich, Marc Thibonnier, and Menachem Shoham

Department of Biochemistry, Case Western Reserve University, Cleveland, Ohio (N.W., R.M.-D., S.N., Z.X., M.S.); Department of Pharmacology, Vanderbilt University, Nashville, Tennessee (S.M.H., S.A.V., V.V.G.); and Department of Medicine, Case Western Reserve University, Cleveland, Ohio (M.T.)

Received September 9, 2005; accepted March 30, 2006

ABSTRACT

Signal transduction by G protein-coupled receptors (GPCRs) is mediated by interactions between intracellular proteins and exposed motifs on the cytoplasmic face of these receptors. Arrestins bind to GPCRs and modulate receptor function either by interfering with heterotrimeric G protein signaling or by serving as signaling adaptors themselves. Calmodulin interacts with GPCRs triggering a calcium response. We have studied the interaction of arrestin2 and calmodulin with intracellular elements of the human V1-vascular vasopressin receptor (hV1R). For this purpose, we designed, expressed, and purified soluble fusion proteins with the maltose-binding protein (MBP) from *Escherichia coli* that mimic the intracellular surface of the hV1R. These MBP fusion proteins bind arrestin2 and calmodulin with affinities in the micromolar range. A different series of soluble receptor analogs, named vasopressin receptor 1 elements on a soluble scaffold (V1ROSS) proteins, consist of the third intracellular loop and/or the C-terminal segment of the hV1R receptor juxtaposed on the surface of the MBP. V1ROSS proteins bind calmodulin and a truncated, phosphorylation-independent form of arrestin2 more tightly than the corresponding linear fusion proteins. Thus, embedding receptor loops within the three-dimensional structure of the MBP yields a better representation of the active conformation of these receptor loops than linear receptor peptides fused onto the C terminus of the MBP. V1ROSS proteins provide a valuable tool to study receptor interactions because they are more amenable to structural analysis than the native membrane receptor. These findings set the stage for the detailed structural analysis of these protein-protein interactions that are important for understanding the mechanism of signaling.

Arginine vasopressin is a cyclic nonapeptide hormone, which modulates various physiological functions such as water reabsorption in the kidneys, blood volume, blood pressure, cellular proliferation, and adrenocorticotropic hormone secretion via its antidiuretic and mitogenic actions (Thibonnier et al., 1998b, 2001a). Vasopressin actions are mediated by specific cell surface proteins, which belong to the large family of G protein coupled receptors (GPCRs). There are three subtypes of vasopressin receptors: the V1-vascular, V2-renal, and V3-pituitary receptors. Vasopressin receptors differ in the type of G proteins to which they are coupled. Consequently, they initiate signaling pathways mediated by different second messengers. The V1-vascular receptor is coupled to G_q and produces a mitogenic response, whereas the V2-renal receptor is coupled to G_s and produces an antimitogenic response (Thibonnier et al., 1998a). Human V1R (hV1R) is expressed in various cell types, including vascular smooth muscle cells, hepatocytes, blood platelets, adrenal cortex, kidney, reproductive organs, spleen, adipocytes, brain, and testis, as the product of the same gene undergoing identical splicing (Thibonnier et al., 2001b). Abnormal vasopressin levels may be involved in the pathogenesis of several diseases such as congestive heart failure, nephritic syndrome, liver cirrhosis, and arterial hypertension (Rosenthal et al., 1993; Thibonnier et al., 1998a,b, 2003). Signal transduction via GPCRs involves the following steps: activation of the receptor by ligand binding at the extracellular surface; interaction with the α subunit of heterotrimeric G proteins on the intracellular side, ultimately leading to the dissociation of the GTP-bound α subunit from the $\beta\gamma$ dimer, both of which subsequently interact with various downstream effec-

This work was supported by National Institutes of Health Grants HL-39757 (to M.S. and M.T.) and GM63097 and EY11500 (to V.V.G.).

[1] Current affiliation: Cleveland Clinic Foundation, Cleveland, OH.

Article, publication date, and citation information can be found at http://molpharm.aspetjournals.org.
doi:10.1124/mol.105.018804.

ABBREVIATIONS: GPCR, G protein-coupled receptor; hV1R, human V1-vascular vasopressin receptor; MBP, maltose-binding protein; V1ROSS, V1-vascular vasopressin receptor elements on a soluble scaffold; IPTG, isopropyl β-D-thiogalactoside; DTT, dithiothreitol; MES, 2-(*N*-morpholino)ethanesulfonic acid; PAGE, polyacrylamide gel electrophoresis; PVDF, polyvinylidene diflouride; ANOVA, analysis of variance.

tors. Arrestins play an important role in the desensitization of GPCRs by interacting with activated and phosphorylated receptors to block further G protein activation (Carman and Benovic, 1998; Gurevich and Gurevich, 2004). The arrestin-receptor complex is then internalized, and the receptor is either dephosphorylated and recycled back to the plasma membrane or degraded by lysosomes. Recent evidence suggests that arrestins also serve as signaling intermediates without the involvement of G proteins (Lefkowitz and Shenoy, 2005). There are four distinct forms of arrestins in mammals. Arrestin1 (visual arrestin) and arrestin4 (cone arrestin) are predominantly expressed in rod and cone photoreceptors, where they regulate the signaling of rhodopsin and cone opsins (Vishnivetskiy et al., 2004). The nonvisual arrestins, arrestin2 (β-arrestin1) and arrestin3 (β-arrestin2), modulate the activity of hundreds of other GPCRs. Detailed mechanistic understanding of the interaction of arrestins with their cognate receptors is important for the elucidation of the structural basis of the receptor specificity and other functional properties of arrestin proteins.

Calmodulin is a ubiquitous intracellular calcium sensor in eukaryotes that undergoes dramatic conformational changes upon Ca^{2+} binding. Calmodulin regulates various cellular proteins, including enzymes, ion channels, transcription factors, and cytoskeletal proteins (Turner et al., 2004). It plays an important role in several GPCR signaling pathways. For example, vasopressin-induced Ca^{2+} increase is involved in water reabsorption by the renal collecting duct. Furthermore, vasopressin-induced trafficking of aquaporin-2 to the cell surface is dependent on calmodulin (Chou et al., 2000). Vasopressin-stimulated cAMP elevation in the inner medullary collecting duct is significantly attenuated in the presence of calmodulin inhibitors, suggesting that calmodulin is required for vasopressin-stimulated adenylyl cyclase activity (Hoffert et al., 2005). A direct interaction between calmodulin and the C terminus of the V2-renal vasopressin receptor has recently been reported (Nickols et al., 2004).

The purpose of developing a soluble mimic of the intracellular part of the receptor is to provide a minimal receptor analog that is easy to purify, stable, and more amenable to structural and functional studies. In this work, we describe the design and preparation of soluble hV1R analogs on a scaffold of the *Escherichia coli* maltose-binding protein (MBP). hV1R intracellular surface elements were attached to the C terminus of MBP. In an attempt to create a more realistic mimic of the hV1R intracellular face, we have subsequently grafted the third intracellular loop of the hV1R as well its C-terminal segment onto the surface of MBP in spatial rather than in sequential proximity to each other. By analogy with the soluble mimics of extracellular elements of the chemokine receptor (Datta and Stone, 2003), we have assigned this vasopressin receptor analog the acronym V1ROSS for vasopressin receptor 1 elements on a soluble scaffold. In this article, we describe the interaction of these soluble hV1R mimics with arrestin2 and calmodulin.

Materials and Methods

Preparation of MBP Fusion Proteins. The DNA sequences corresponding to selected segments of hV1R (NP_000697, National Center for Biotechnology Information protein database) were inserted into a modified pMAL vector (a generous gift from Dr. Cynthia Wolberger, Department of Biophysics and Biophysical Chemistry, Johns Hopkins School of Medicine, Baltimore, MD) between PstI and HindIII restriction sites. The following fragments were inserted: the second extracellular loop (E2, residues 197–215: sense, atgctgcagctgctgcagtcaccaaggcccg; antisense, atcaagctttcaggcacgagaacccca); the second intracellular loop (I2, residues 147–171: sense, atgctgcagctgctgcagccgaccgctacatg; antisense, atcaagctttcagatcatgaggcgcga); the third intracellular loop (I3, residues 240–292: sense, atgctgcagctgctgcatgctacaacatctggtg; antisense, atcggatcctcaagtcatcttcaccgtgc); and the C-terminal tail (Ct, residues 362–418, sense, atgctgcagctgctgctagcttcccagccgcccaaaac; antisense, ataagctttcaagttgaaacaggaatgaatttg). The resulting proteins were named MBP-E2, MBP-I2, MBP-I3, and MBP-Ct correspondingly (Fig. 1). The third intracellular loop and a GGGA short linker were inserted into the MBP-Ct DNA sequence between PstI and NheI restriction sites (sense, atgctgcagctgctgcatgctacaacatctggtg; antisense, atgctagcaccaccacccatcttcaccgtg) to generate a protein having both I3 and Ct, dubbed MBP-I3-GGGA-Ct. MBP with the insertion of five alanines at the C terminus was made to serve as a negative control in binding experiments (sense, acgctgagcgcaggtatta; antisense, ctctgcagtcaagcagcagcagcattagtctgcg). All plasmids were checked by DNA sequencing.

V1ROSS-I3-Ct Construct. MBP-Ct was used as the template to construct V1ROSS-I3-Ct. Mutations K171E, Y172F, I179S, and K180R of MBP were performed with the QuikChange site-directed mutagenesis kit (Stratagene, La Jolla, CA) to introduce EcoRI and XbaI endonuclease digestion sites. The primers for the KY to EF mutation are 5′-ctgacgggggttatgcgttcgaattcgaaaacggcaagtacgacat-3′ and 5′-atgtcgtacttgccgttttcgaattcgaacgcataaccccgtcag-3′. The primers for the IK to SR mutation are 5′-gaaaacggcaagtacgactctagagacgtgggcgtgga-3′ and 5′-tccacgcccacgtctctagagtcgtacttgccgttttc-3′. I3 was amplified by primers 5′-ggaattctgctacaacatctggtgc-3′ and 5′-gctctagaagtcatcttcaccgtgc-3′ and was inserted in between the two mutation sites on MBP-Ct. The V1ROSS-I3-Ct sequence was amplified with primers 5′-aagcatatgatgaaaatcgaagaagg-3′ and 5′-accggatcctcaagttgaaacaggaatgaa-3′ and then inserted into NdeI and BamHI sites on a PET-15b vector (Novagen, Madison, WI) to introduce an N-terminal His-tag into V1ROSS. All plasmids were checked by DNA sequencing.

Purification of His-V1ROSS-I3-Ct. His-V1ROSS-I3-Ct was expressed in *E. coli* BL21 pLysS cells. The expression was induced by adding 1 mM IPTG at the mid-log point of the growth curve for 2 h

MKIEEGKLVIWINGDKGYNGLAEVGKKFEKDTGIKVTVEHPDKLEEKFPQVA
ATGDGPDIIFWAHDRFGGYAQSGLLAEITPDKAFQDKLYPFTWDAVRYNGKL
IAYPIAVEALSLIYNKDLLPNPPKTWEEIPALDKELKAKGKSALMFNLQEPY
FTWPLIAADGGYAFKYENGKYDIKDVGVDNAGAKAGLTFLVDLIKNKHMNAD
TDYSIAEAAFNKGETAMTINGPWAWSNIDTSKVNYGVTVLPTFKGQPSKPFV
GVLSAGINAASPNKELAKEFLENYLLTDEGLEAVNKDKPLGAVALKSYEEEL
AKDPRIAATMENAQKGEIMPNIPQMSAFWYAVRTAVINAASGRQTVDAALAA
AQTNAAAAA-**hV1R insert**

hV1R insert

E2 VTKARDCWATFIQPWGSRA
I2 ADRYIAVCHPLKTLQQPARRSRLMI
I3 CYNIWCNVRGKTASRQSKGAEQAGVAFQKGFLLAPCVSSV
KSISRAKIRTVKM
Ct SFPAAQNMKEKFNKEDTDSMSRRQTFYSNNRSPTNSTGM
WKDSPKSSKSIKFIPVST
I3-GGGA-Ct CYNIWCNVRGKTASRQSKGAEQAGVAFQKGFLLAPCVSSV
KSISRAKIRTVKMGGGASFPAAQNMKEKFNKEDTDSMSRR
QTFYSNNRSPTNSTGMWKDSPKSSKSIKFIPVST

Fig. 1. Design of MBP fusion proteins with various inserts of hV1R segments. The amino acid sequence of the fusion proteins is shown in one-letter code. Three charged amino acids on the C-terminal helix of MBP were mutated to alanines (underlined) to stabilize the helix. The engineered penta-alanine linker between MBP and the inserts is shown in italics. Cysteines 365 and 366, which are palmitoylated in the hV1R, were mutated to alanines (underlined).

at 37°C with shaking at 250 rpm. Cells were harvested by centrifugation at 6000 rpm and resuspended in column buffer (50 mM sodium phosphate, pH 7.4, and 1 M NaCl), containing a tablet of protease inhibitor cocktail (Roche Diagnostics, Indianapolis, IN). The protein was released from cells by sonication, and the cell debris was removed by centrifugation. The supernatant was loaded onto a Hitrap HP 1-ml column (GE Healthcare, Little Chalfont, Buckinghamshire, UK) at 1 ml/min, and the column was washed with column buffer to a stable baseline. The column was further washed with 20 mM imidazole in column buffer to remove proteins bound nonspecifically. The target protein was eluted with a linear gradient of 20 to 300 mM imidazole. The fractions containing the target protein were pooled and dialyzed into MonoS column buffer (50 mM MES, pH 6.5, 0.1 M NaCl, 1 mM DTT, and 1 mM EDTA). The dialyzed protein solution was loaded onto a MonoS 4.6/100PE column (GE Healthcare) at a rate of 1 ml/min. The protein was eluted with a linear gradient of 0.1 to 0.6 M NaCl. The fractions containing the target protein in the purest form were pooled, concentrated to small volume, and loaded onto a Sephadex S200 10/300 GL sizing column (GE Healthcare) at a rate of 0.5 ml/min. The protein was eluted with 50 mM sodium phosphate, pH 7.5, and 150 mM NaCl. The purified protein fractions were pooled and dialyzed into His-tag pull-down assay buffer (20 mM HEPES, pH 7.5, 0.1 M NaCl, and 1 mM DTT).

Design and Purification of His-V1ROSS-I3. V1ROSS DNA was used as the template for the construction of His-V1ROSS-I3, which contains only the I3 loop of hV1R on the surface of MBP at the same position as in V1ROSS-I3-Ct. The sequence of V1ROSS-I3 was amplified by primers 5′-aagcatatgatgaaaatcgaagaagg-3′ and 5′-accggatcctcacattagtctgcgcggctg-3′ and then inserted into NdeI and BamHI sites on a PET-15b vector (Novagen) to generate His-V1ROSS-I3. The plasmid was checked by DNA sequencing. His-V1ROSS-I3 was expressed in *E. coli* BL21 pLys S cells, induced with 1 mM IPTG at the midpoint of growth curve for 2 h at 37°C. The purification of His-V1ROSS-I3 was similar to His-V1ROSS. The soluble proteins mixture was first purified by Hitrap HP column. The fractions containing most pure target protein were pooled and dialyzed into 50 mM MES buffer, pH 6.2., and loaded onto Mono S column. The protein was eluted with 0 to 0.3 M NaCl gradient after column wash. Purified His-V1ROSS-I3 was used for the calmodulin pull-down binding assay and fluorescence experiments.

Purification of Arrestin2. Arrestin2 was expressed and purified according to Gurevich and Benovic (2000). In brief, *E. coli* BL21, inoculated with stock cells, was incubated at 30°C overnight with shaking at 250 rpm. Protein expression was induced with 30 μM IPTG for 4 h at 30°C. The cell pellet was suspended in lysis buffer (50 mM Tris-HCl, pH 8.0, 5 mM EGTA, 5 mM EDTA, 1 mM DTT, 1 mM phenylmethylsulfonyl fluoride, 10 μM leupeptin, 2 mM benzamidine, 0.7 μg/ml pepstatin, and 5 μg/ml chymostatin) with the addition of 0.1 mg/ml lysozyme. The cells were broken by a freeze-thaw cycle and sonication. Cell debris was removed by centrifugation. Ammonium sulfate (0.32 mg/ml) was added to the supernatant, and precipitated protein was pelleted by centrifugation. The resulting precipitate was redissolved in column buffer (10 mM Tris-HCl, pH 7.5, 2 mM EDTA, 2 mM EGTA, 2 mM benzamidine, 1 mM phenylmethylsulfonyl fluoride, 10 μM leupeptin, 2 mM benzamidine, 0.7 μg/ml pepstatin, and 5 μg/ml chymostatin) and loaded onto a 25-ml pre-equilibrated Heparin-Sepharose column. The protein was eluted with a 0.1 to 1 M NaCl linear gradient. The fractions containing the target protein were pooled and loaded onto a 10-ml pre-equilibrated Q-Sepharose column. The protein was eluted with a 0.1 to 1 M NaCl linear gradient. The fractions containing the purified arrestin2 were pooled, further purified on a Sephadex S75 column (GE Healthcare), concentrated, and stored at −80°C.

MBP Pull-Down Binding Assay. Wet cells (0.5 g) of each MBP fusion protein (MBP-E2, MBP-I2, MBP-I3, MBP-Ct, and MBP-I3-GGGA-Ct) were suspended in 2 ml of binding buffer (20 mM Tris-HCl, pH 7.5, 0.1 M NaCl, 1 mM EDTA, and 1 mM DTT) at 4°C and sonicated on ice to release the proteins. An EDTA-free tablet of protease inhibitor cocktail (Roche Diagnostics) was added to the suspension to prevent proteolysis. The solutions were spun down at 4°C. The supernatant was diluted 5-fold and incubated with pre-equilibrated amylose resin (50 μl of resin for each fusion protein; New England Biolabs, Beverly, MA) at 4°C with gentle shaking for 1 h. The resin was subsequently washed with binding buffer until the absorbance at 280 nm was less than 0.05. The washed and protein-bound amylose resin was incubated with 1 μg of purified arrestin2 (full-length and 1–382 truncated form) at 4°C for 1 h with gentle shaking. The resin was spun down at 500*g* for 1 min after incubation in the mini-spin separation column to remove free arrestin2. The resin was washed twice with 0.5 ml of binding buffer. The washed resin was transferred into clean Eppendorf tubes. SDS sample buffer was added, and the resin was boiled for 5 min to release the bound proteins. Samples were analyzed by 10% SDS-PAGE and transferred onto a PVDF membrane by a semidry transfer method, followed by blocking overnight with Tris-buffered saline/Tween/5% milk. The PVDF membrane was incubated with an anti-arrestin2 antibody at 1:10,000 dilution for 1 h at ambient temperature with gentle shaking. The PVDF membrane was washed extensively and incubated with peroxidase-labeled anti-rabbit IgG (Vector Laboratories, Burlingame, CA) for 1 h at ambient temperature with gentle shaking. The PVDF membrane was washed with Tris-buffered saline/Tween buffer and then incubated with SuperSignal West Pico Chemiluminescent Substrate (Pierce Chemical, Rockford, IL). The PVDF membrane was then exposed to CL-XPosure film (Pierce Chemical).

Cobalt Metal Affinity Pull-Down Assay. Purified His-V1ROSS (0.5 nmol) was incubated with 50 μl of Talon affinity resin (Clontech, Mountain View, CA) for 1 h at 4°C with gentle shaking. The resin was washed with binding buffer (20 mM HEPES, pH 7.5, 0.1 M NaCl, and 1 mM DTT) and incubated with 0.1 nmol of full-length arrestin2 or arrestin2 (1–382) at 4°C for 1 h with gentle shaking. Free arrestin2 was removed on a mini-spin separation column, followed by washing twice with 0.5 ml of binding buffer. The washed resin was transferred to clean Eppendorf tubes, SDS sampling buffer was added, and the solution was boiled. The samples were loaded onto SDS-PAGE and transferred to a PVDF membrane. The proteins were detected by immunoblotting with anti-arrestin2.

Calmodulin-Agarose Pull-Down Assay for Receptor Analogs. Calmodulin-agarose (Sigma-Aldrich, St. Louis, MO) was washed in binding assay buffer (20 mM Tris-HCl, pH 7.5, and 0.1 M NaCl) and incubated with purified MBP (negative control), MBP-I3, and His-V1ROSS-I3 in the presence of 0.1 mM $CaCl_2$ or 5 mM EGTA at 4°C. The resin was washed in a mini-spin column to remove unbound and nonspecifically bound proteins. Specifically bound proteins were eluted with SDS sample buffer and analyzed by SDS-PAGE. The protein was detected by immunoblotting with anti-MBP (New England Biolabs).

Fluorescence Measurement of Dansyl-Arrestin2. Purified arrestin2 was conjugated with dansyl chloride (Invitrogen, Carlsbad, CA) in 50 mM sodium phosphate, pH 7.5, and 150 mM NaCl at 4°C for 2 h. One microgram of dansyl chloride was used for every 10 μg of protein. Free dye was removed by extensive dialysis into binding buffer (20 mM Tris-HCl, pH 7.5, and 0.1 M NaCl). The degree of labeling was determined as described in the product information for amine-reactive probes from Invitrogen. Dansyl-arrestin2 (1 μM for full-length and 1.5 μM for 1 to 382 truncated form) was incubated with increasing concentrations of MBP-I3, MBP-Ct, MBP-I3-GGGA-Ct, and His-V1ROSS-I3-Ct overnight, respectively. The solution was excited at 340 nm, and the fluorescence emission spectra were measured in the wavelength range of 400 to 650 nm on an SLM 8000C spectrofluorimeter (SLM Instruments, Rochester, NY). The integral under the fluorescence curve was plotted against concentrations of each fusion protein, and the data were fitted to a Boltzmann sigmoidal function with the Prism 4 software (GraphPad Software Inc., San Diego, CA). The dissociation constant was calculated according to Bertrand et al. (1994). In brief, the fractional degree of saturation of dansyl-arrestin2 was determined by $a = (F - F_0)/(F_\infty - F_0)$, where F_0

is the fluorescence signal of dansyl-arrestin2 itself, and F_∞ is the fluorescence signal at saturation level; $1/(1 - a)$ was plotted against the concentration of fusion proteins divided by a. The data of this plot were fitted to a straight line by linear regression. K_d was determined from the reciprocal of the slope.

Dansylation of Calmodulin. Fifty microliters of calmodulin (Calbiochem, San Diego, CA) at a concentration of 10 mg/ml was incubated with 5 μl of 10 mg/ml dansyl chloride (Invitrogen) at 4°C for 5 h in 20 mM Tris-HCl, pH 7.5, 0.1 M NaCl, and 0.1 mM $CaCl_2$. Free dansyl chloride was removed by extensive dialysis. The extent of labeling was 50% as determined by absorbance at 340 nm according to Molecule Probes' product information. Dansyl-calmodulin (4.3 μM) was incubated with increasing concentrations of MBP-I3 and His-V1ROSS-I3 (0–40 μM) at 4°C overnight. The fluorescence emission spectrum of each solution was measured in the wavelength range of 400 to 650 nm after excitation at 340 nm. Dissociation constants were calculated by the method described above.

Results

Design of MBP Fusion Proteins with Various hV1R Inserts. The MBP, widely used as an affinity and solubility tag in structural biology, served as a soluble scaffold to which various segments of the hV1R were linked to its C terminus. A penta-alanine linker was engineered in between MBP and an hV1R segment, as described previously (Ke and Wolberger, 2003). Five different hV1R segments were fused to MBP: E2, I2, I3, Ct, and a linear combination of I3 and Ct of the human V1R (Fig. 1). These five fusion proteins are designated MBP-E2, MBP-I2, MBP-I3, MBP-Ct, and MBP-I3-GGGA-Ct. The GGGA spacer between I3 and Ct was designed to span the distance between transmembrane helices 5 and 6, as measured in the crystal structure of rhodopsin (Palczewski et al., 2000) (Protein Data Bank code 1F88). Three charged residues at the C terminus of MBP were mutated to alanines to stabilize the C-terminal helix of MBP. All the MBP fusion proteins were expressed in *E. coli* BL21 pLysS cells and purified by amylose affinity chromatography. The purity varied between 80 and 95% for the different fusion proteins, as judged by SDS-PAGE (data not shown).

Binding of MBP Fusion Proteins to Arrestin2. The five MBP fusion proteins were incubated with arrestin2, loaded onto an amylose-affinity column and eluted with SDS sample buffer. Bound arrestin2 was detected by Western blotting with an anti-arrestin2 antibody. MBP fusion proteins containing either I3, Ct or both I3 and Ct bind to full-length arrestin2, whereas MBP fusion proteins containing E2 or I2 do not (Fig. 2A). To probe the effects of receptor phosphorylation on arrestin2 binding, an identical set of experiments was carried with a truncated form of arrestin2 (residues 1–382). This form of arrestin2 binds to receptors independent of their phosphorylation state (Gurevich et al., 1997). The results with truncated arrestin2 were identical except that MBP-I2 displayed weak, but detectable arrestin2 (1–382) binding (Fig. 2B). A negative control for nonspecific binding to the MBP fusion proteins was carried out with an unrelated protein, transcription factor TAFII:7, which did not bind to any of the MBP fusion proteins, as determined with a specific antibody to TAFII:7 (data not shown).

Design of V1ROSS Proteins. To create a better soluble mimic of the hV1R, we engineered I3 and Ct on the surface of MBP in a way that incorporates the receptor elements into the three-dimensional structure of MBP. We hypothesized that this design would yield a more stable protein that more closely mimics the intracellular surface of the hV1R. Based on the examination of the MBP crystal structure (Protein Data Bank code 1ANF) we selected three interacting helices (6 and 7 and the C-terminal helix of MBP) as the attachment points for receptor elements. The loop connecting helices 6 and 7 (residues 169 to 180) was replaced with I3, and the sequence of Ct was inserted at the C terminus of MBP after a penta-alanine linker (Fig. 3). Molecular modeling suggested that I3 and Ct would be displayed on the surface of this engineered protein in a manner mimicking the relative orientation of I3 and Ct on the cytoplasmic surface of the intact hV1R.

Similar to our linear design, we introduced three alanine substitutions (E359A, K362A, and D363A) into MBP to stabilize the C-terminal helix. The V1ROSS proteins were expressed in *E. coli*. Affinity purification on an amylose column could not be carried out, because V1ROSS-I3 and V1ROSS-I3-Ct did not bind to the amylose resin, presumably as a result of impaired carbohydrate-binding capacity. To facilitate affinity purification, a removable N-terminal His_6-tag was introduced in a subsequent design by subcloning the entire sequence into a pET15b vector (Novagen). This His-tagged V1ROSS-I3-Ct protein was expressed in *E. coli* and isolated at >95% purity after nickel-affinity, ion exchange and gel filtration chromatography. This purified His-V1ROSS-I3-Ct protein was used for all subsequent qualitative and quantitative binding assays.

Binding of His-V1ROSS-I3-Ct to Arrestin2. His-V1ROSS-I3-Ct binds to both full-length and truncated arrestin2 (1–382), as demonstrated by a cobalt metal affinity pull-down assay with an anti-arrestin2 antibody (Fig. 4). Thus, receptor surface elements embedded in V1ROSS are available for interaction with arrestin2. These results are similar to the pull-down assays with linear MBP fusion proteins, but the affinity of truncated arrestin2 (1–382) to His-V1ROSS-I3-Ct is higher than for the linear MBP fusion proteins, as measured by fluorescence enhancement (data shown below).

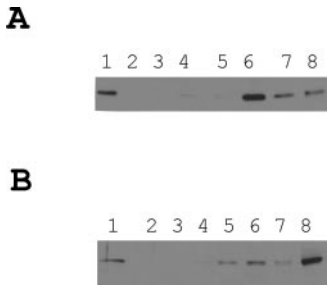

Fig. 2. Anti-arrestin2 immunoblots on an amylose affinity column. A, pull-down binding assay with full-length arrestin2. Full-length arrestin2 was loaded onto an amylose column after equilibration with various MBP fusion proteins. The columns were washed after arrestin2 loading and eluted with SDS sample buffer. The eluents were analyzed by Western blot with an anti-arrestin2 antibody. Lanes 1 and 2 are full-length arrestin2 and MBP as positive and negative controls for the specificity of the antibody, respectively. Lane 3 is MBP, lane 4 is MBP-E2, lane 5 is MBP-I2, lane 6 is MBP-I3, lane 7 is MBP-Ct, and lane 8 is MBP-I3-GGGA-Ct. MBP fusion proteins containing I3, Ct, or the combination of I3 and Ct (lanes 6–8) exhibit binding to full-length arrestin2. B, pull-down binding assay with a phosphorylation-independent truncated form of arrestin2 (residues 1–382). The lanes are analogous to those in A. The results are identical to full-length arrestin2 except that MBP-I2 (lane 5) exhibits weak binding. The presence of both I3 and Ct seems to strengthen binding to arrestin2.

Proteins Containing the Sequence of the Third Intracellular Loop of the hV1R Bind to Calmodulin/Ca^{2+}. Calmodulin is known to interact directly with the V2 vasopressin receptor (Nickols et al., 2004). To test whether calmodulin might interact with the hV1R as well, a search at the Calmodulin Target Database (http://calcium.uhnres.utoronto.ca/ctdb/pub_pages/general/index.htm) was performed against the hV1R sequence. The search predicted a binding site at the C terminus of the I3 loop of the hV1R (residues 282–295). Using a pull-down assay on a calmodulin-agarose column we found that MBP-I3 binds to calmodulin in a Ca^{2+}-dependent manner (Fig. 5), suggesting that the calmodulin-binding-site on hV1R is located on I3. To further test this hypothesis, we designed a soluble mimic of just the I3 loop of hV1R, His-V1ROSS-I3. A design similar to His-V1ROSS-I3-Ct was used to produce a soluble mimic of just the I3 loop of hV1R, His-V1ROSS-I3. As shown in Fig. 5, His-V1ROSS-I3 binds to calmodulin-agarose in the presence but not in the absence of Ca^{2+}, demonstrating that the calmodulin-binding sequence is localized on the I3 loop, and that this loop in the His-V1ROSS-I3 protein is accessible to calmodulin.

Affinity Measurements. Next, we determined the affinity of these protein-protein interactions using fluorescence enhancement of dansyl-labeled proteins as a readout. Ligand binding to dansyl-labeled protein is thought to shield the fluorophore from the aqueous environment, and this can be detected by an enhancement in the fluorescence emission. Arrestin2 (both full-length and 1–382 truncated form) was labeled with dansyl chloride. The fluorescence signal of dansyl-arrestin2 increased with the addition of fusion proteins. The addition of His-V1ROSS-I3-Ct to dansyl arrestin2 (1–382) induced a greater change in fluorescence than other fusion proteins at the same concentration (Fig. 6A), and the binding curve has a steeper initial slope (Fig. 6C). Titration of the full-length dansyl arrestin2 with fusion proteins yielded binding curves with almost identical initial slopes (Fig. 6D), although His-V1ROSS-I3-Ct yielded the highest fluorescence enhancement (Fig. 6, B and D). The dissociation constants were calculated from these measurements according to Bertrand et al. (1994), and the results are shown in Table 1. It is noteworthy that the affinity of wild-type arrestin2 for all the constructs tested is similar (K_d in the 0.5–2 μM range), whereas the more conformationally "loose" truncated form demonstrates essentially the same affinity as full-length for the V1ROSS-I3-Ct construct (which seems to be the closest mimic of the cytoplasmic receptor surface) and lower affinity for the other constructs. Both linear mimics

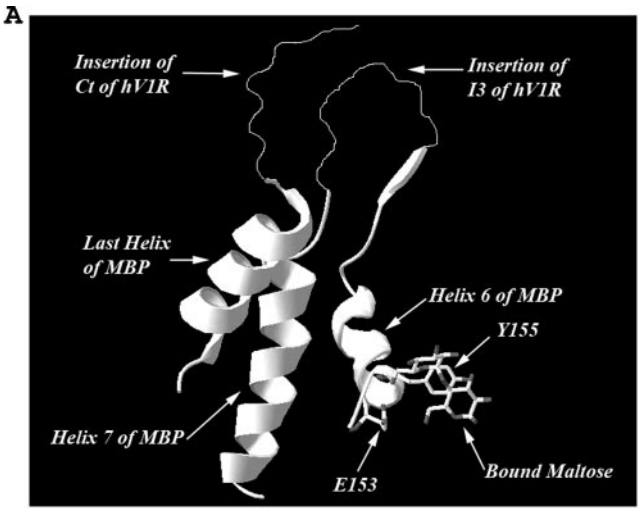

B

*MGSSHHHHHHSSGLVPRGSHM*MKIEEGKLVIWINGDKGYNGLAEVGKKFE
KDTGIKVTVEHPDKLEEKFPQVAATGDGPDIIFWAHDRFGGYAQSGLLAE
ITPDKAFQDKLYPFTWDAVRYNGKLIAYPIAVEALSLIYNKDLLPNPPKT
WEEIPALDKELKAKGKSALMFNLQEPYFTWPLIAADGGYAFEF**CYNIWCN**
VRGKTASRQSKGAEQAGVAFQKGFLLAQCVSSVKSISRAKIRTVKMSRDV
GVDNAGAKAGLTFLVDLIKNKHMNADTDYSIAEAAFNKGETAMTINGPWA
WSNIDTSKVNYGVTVLPTFKGQPSKPFVGVLSAGINAASPNKELAKEFLE
NYLLTDEGLEAVNKDKPLGAVALKSYEEELAKDPRIAATMENAQKGEIMP
NIPQMSAFWYAVRTAVINAASGRQTVDAALAAAQTN*AAAAA***SFPAAQNMK**
EKFNKEDTDSMSRRQTFYSNNRSPTNSTGMWKDSPKSSKSIKFIPVST

Fig. 3. Design of the V1ROSS-I3-Ct protein. A, amino acid sequences corresponding to I3 and Ct were inserted in between three adjacent helices of MBP. Bound maltose is depicted in ball-and-stick representation. B, amino acid sequence of His-V1ROSS-I3-Ct. The His_6-tag and a thrombin-digestive site from the PET 15b vector are in italics. Two mutations, EF (mutated from KY) and SR (mutated from IK), engineered to introduce EcoRI and XbaI sites, are underlined. The sequence between EF and SR, shown in bold, corresponds to I3 of hV1R. The penta-alanine linker is in italics, followed by the sequence corresponding to Ct of hV1R, shown in bold, with Cys365 and Cys366 mutated to alanines (underlined).

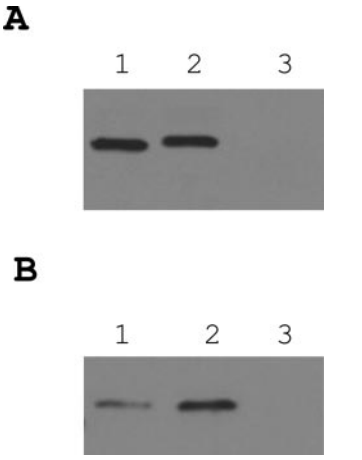

Fig. 4. Anti-arrestin2 immunoblots of cobalt metal affinity column (TALON) eluents. A, His-V1ROSS-I3-Ct was loaded onto the cobalt affinity column followed by passing arrestin2 (1–382) over the column. Elution was performed with denaturing SDS sample buffer. The eluent was analyzed by immunoblotting with an anti-arrestin2 antibody (lane 1). Lanes 2 and 3 are truncated arrestin2 (1–382) and MBP as positive and negative control for antibody specificity, respectively. B, same as A, except with full-length arrestin2.

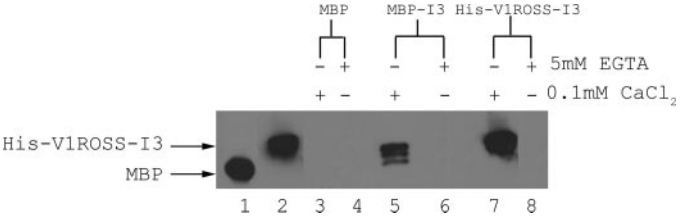

Fig. 5. Anti-MBP immunoblots of calmodulin-agarose column eluents. Lanes 1 and 2 are MBP and His-V1ROSS-I3 as controls for the antibody specificity. Fusion proteins were incubated with calmodulin-agarose in the presence of 0.1 mM Ca^{2+} or 5 mM EGTA. The bound proteins were eluted with SDS sampling buffer after extensive column wash. The eluents were analyzed by immunoblotting with anti-MBP antibody. MBP-I3 and His-V1ROSS-I3 migrated differently from MBP because of the addition of the 5.7-kDa I3 insert.

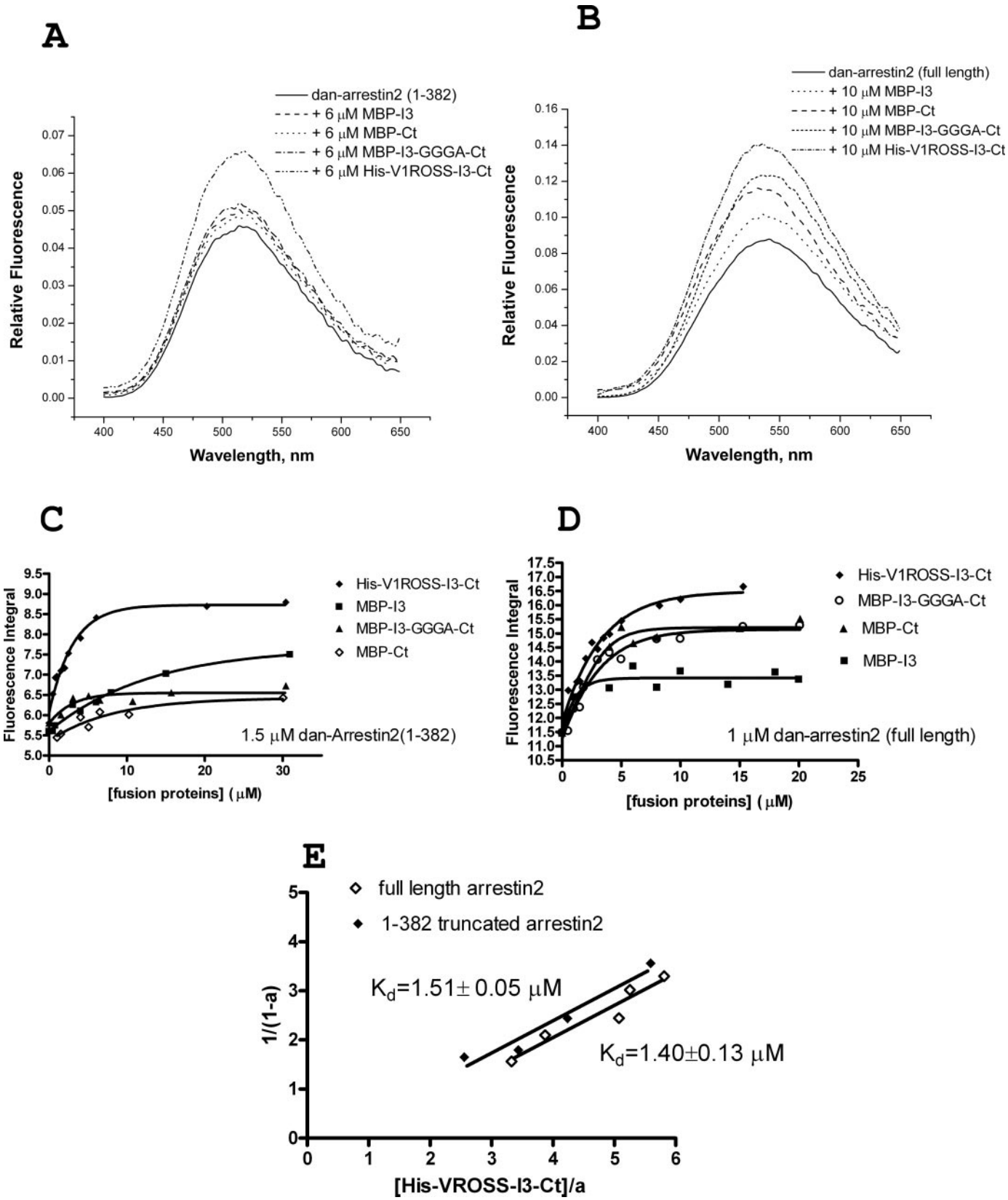

Fig. 6. Fluorescence emission spectra of dansyl-arrestin2 in the presence of various MBP fusion proteins. A and B, fluorescence emission spectra of dansyl-arrestin2 and increasing concentrations of various fusion proteins. C and D, integrated area under the fluorescence curve is plotted against the concentration of the fusion proteins. The data were fitted to a Boltzmann sigmoidal equation. E, analysis of the data in C and D according to Bertrand et al. (1994). Fractional degree of saturation of dansyl-arrestin2 was determined as $a = (F - F_0)/(F_\infty - F_0)$, where F_∞ is fluorescence at saturation level; $1/(1 - a)$ was plotted against the concentration of His-VROSS-I3-Ct divided by a. The reciprocal of the slope is the dissociation constant (K_d).

containing I3 have essentially the same K_d, whereas the receptor C terminus alone demonstrates dramatically lower affinity for this arrestin2 mutant.

Affinities of MBP-I3 and His-V1ROSS-I3 for calmodulin were determined by fluorescence enhancement of dansyl calmodulin. Increasing concentrations of MBP-I3 and His-V1ROSS-I3 were incubated with 4.3 μM dansyl calmodulin, and fluorescence emission spectrum was acquired for each solution. The fluorescence signal of dansyl calmodulin increased with the addition of MBP-I3 and His-V1ROSS-I3, and the observed enhancement is substantially greater for His-V1ROSS-I3 than for MBP-I3 (Fig. 7, A and B). The dissociation constants for calmodulin binding to MBP-I3 and His-V1ROSS-I3 were calculated to be 12.54 ± 0.61 and 1.87 ± 0.12 μM, respectively (Fig. 7C; Table 1).

Discussion

Structural information on GPCRs and their complexes with interacting proteins is crucial for understanding their signaling mechanisms. More than half of marketed drugs target GPCRs, but little structural information is available on GPCRs because of the difficulties in preparing milligram quantities of pure and active receptor and the formidable task of crystallizing membrane proteins. The only GPCR crystal structures determined so far are those of the inactive nonsignaling form of bovine rhodopsin (Palczewski et al., 2000; Okada et al., 2002; Li et al., 2004). Moreover, the rhodopsin crystal structure lacks crucial information on elements that bind intracellular proteins, because some of the loops connecting the transmembrane domains are not well ordered and have somewhat different conformations in different structures. Therefore, receptor analogs that preserve the signaling protein-binding properties of GPCRs would be very useful for studying receptor interactions with cytoplasmic partners. In this work, we designed, expressed, purified, and functionally characterized soluble analogs of the intracellular face of the hV1R. First, various intracellular elements of hV1R were fused to the C terminus of MBP, a stable bacterial protein that is used as a tag for expression, affinity purification and crystallization of proteins (Ke and Wolberger, 2003). In these fusion proteins, the elements of the protein of interest were connected to MBP by a short linker (usually several alanines), and charged residues in the C-terminal helix of MBP were mutated to alanines to stabilize the helix. We have used this methodology to prepare several MBP fusion proteins containing intracellular segments of the hV1R.

In a second generation design of soluble receptor analogs, we engineered I3 and Ct of the hV1R in spatial proximity, as one would predict for the intact receptor. MBP was again used as a scaffold, but in this design a loop in MBP was replaced with I3, and the Ct was attached to the C terminus of MBP. In this way, I3 and Ct were grafted onto three adjacent helices of MBP (Fig. 3A). This engineered receptor analog was assigned the acronym V1ROSS by analogy to the chemokine receptor analog CROSS (Datta and Stone, 2003). In CROSS, the N terminus and the third extracellular loop of the chemokine receptor 3 were grafted onto the surface of the B1 domain of Streptococcal protein G. CROSS was found to bind the ligand eotaxin, and it competed with the chemokine receptor 3 for eotaxin binding.

All receptor analogs used in this study that contain either I3 or Ct moieties of the hV1R do interact with the truncated and full-length forms of arrestin2. The linear receptor analogs (MBP-I3-GGGA-Ct and MBP-I3) display higher affinity for arrestin2 (1–382) than MBP-Ct. This finding is in agreement with a report that a cyclic peptide mimicking I3 of the V2 receptor inhibits signaling (Granier et al., 2004). We also found that truncated arrestin2 demonstrates the highest affinity for V1ROSS-I3-Ct, which was designed to have I3 and Ct moieties in spatial proximity. This finding suggests that both receptor elements in proper orientation provide the surface for multisite arrestin binding in intact GPCRs (Gurevich and Benovic, 1993; Gurevich and Gurevich, 2004; Lefkowitz and Shenoy, 2005). Wild-type arrestin2 demonstrates similar affinity for these constructs. It is noteworthy that the affinity of wild-type and truncated arrestin2 for the closest receptor analog V1ROSS-I3-Ct is virtually the same (Table 1).

The receptor analog containing the I2 loop displayed weak

TABLE 1

Affinity of various hV1R analogs for arrestin2 and calmodulin

Means ± S.E.M. of three measurements of the dissociation constants are presented. Calmodulin affinity for V1ROSS-I3 was higher than for MBP-I3, as determined by ANOVA (StatView software; SAS Institute, Cary, NC). The data for both arrestins were first analyzed by two-way ANOVA with arrestin and construct as main factors. The effects of both arrestin [$F(1,16) = 72.5$; $P < 0.0001$] and construct [$F(3,16) = 35.6$; $P < 0.0001$] were significant. We also found significant interaction between the two factors [$F(3,16) = 38.8$; $P < 0.0001$]. Therefore, the data for each type of arrestin were further analyzed by one-way ANOVA with construct as main factor. We found no significant differences in the affinity of full-length arrestin2 for the four constructs tested. In truncated arrestin2, the effect of the construct was significant [$F(93,8) = 37.7$; $P < 0.0001$]. Post hoc comparison of means with Bonferroni correction for multiple comparisons demonstrated that the affinity of truncated arrestin for all other constructs was higher than for MBP-Ct. The affinity of full-length arrestin2 for every construct except V1ROSS-I3-Ct was found to be higher than that of truncated arrestin2 (1–382). Both arrestins demonstrated equally high affinity for V1ROSS-I3-Ct.

	K_d		
	Calmodulin	Full-Length Arrestin2	Truncated Arrestin2 (1–382)
		μM	
MBP-I3	12.54 ± 0.61	1.33 ± 0.59*	6.62 ± 0.42**
MBP-Ct	N.D.	0.66 ± 0.10*	41.55 ± 5.72
MBP-I3-GGGA-Ct	N.D.	1.70 ± 0.38***	6.91 ± 1.78**
V1ROSS-I3-Ct	N.D.	1.40 ± 0.13	1.51 ± 0.05**
V1ROSS-I3	1.87 ± 0.12†	N.D.	N.D.

N.D., not determined.
* $P < 0.01$.
** $P < 0.001$.
*** $P < 0.05$.
† $P < 0.0001$.

binding to truncated arrestin2 (1–382) in the pull-down assays. This finding suggests that I2 also contributes to a noncontiguous arrestin-binding site on the intracellular face of GPCRs. The rhodopsin I2 loop has been implicated in arrestin interaction by mutagenesis (Raman et al., 2003) and peptide inhibition (Krupnick et al., 1994). I2 of the hV1R has been shown to be critical in selective activation of G proteins (Liu and Wess, 1996).

The fact that receptor analogs carrying I2, I3, or Ct moieties bind arrestin2 is consistent with the importance of these loops for arrestin binding to many different GPCRs (Krupnick et al., 1994; Mukherjee et al., 1999b; Nakamura et al., 2000; Potter et al., 2002; Raman et al., 2003). These intracellular receptor segments also contain G protein-coupled receptor kinase phosphorylation sites. Ct is phosphorylated by GRK5 and protein kinase C and plays an important role in receptor trafficking (Berrada et al., 2000; Thibonnier et al., 2001b). I3 of the hV1R also contains a protein kinase C consensus motif [(S/T)X(R/K)]. Binding of full-length arrestin2 to the unphosphorylated receptor analogs in vitro in this work suggests that arrestin2-mediated signaling can occur without the involvement of receptor phosphorylation, as has been shown for the luteinizing hormone receptor and several other GPCRs (Mukherjee et al., 1999a; for review, see Gurevich and Gurevich, 2006).

The soluble receptor mimics used in this study display relatively weak binding to arrestin2 in the micromolar range. Even arrestin2 affinity for V1ROSS-I3-Ct is lower than the reported nanomolar affinities of both nonvisual arrestins for purified reconstituted β2-adrenergic and m2 muscarinic cholinergic receptors (Gurevich et al., 1995, 1997). Taking into account that arrestin2 expression in many cells, especially mature neurons, reaches 0.2 μM, approximately the same as the concentration of GPCRs (Gurevich et al., 2004), a dissociation constant of approximately 1 μM means that only approximately 20% of receptors would be bound to arrestin2 at equilibrium. However, the affinity of arrestin2 to intact GPCRs has been reported to range from 0.2 to 5 nM (Gurevich et al., 2004), approximately 3 orders of magnitude higher than for the soluble receptor mimics in this study. The reason for the tighter binding to intact receptors could be the involvement of receptor moieties other than I3 and Ct in arrestin2 binding. Furthermore, tight binding of arrestin2 requires activated receptors, whereas the soluble receptor mimics used in this study may not represent the activated conformation of receptor elements. Consequently, binding to

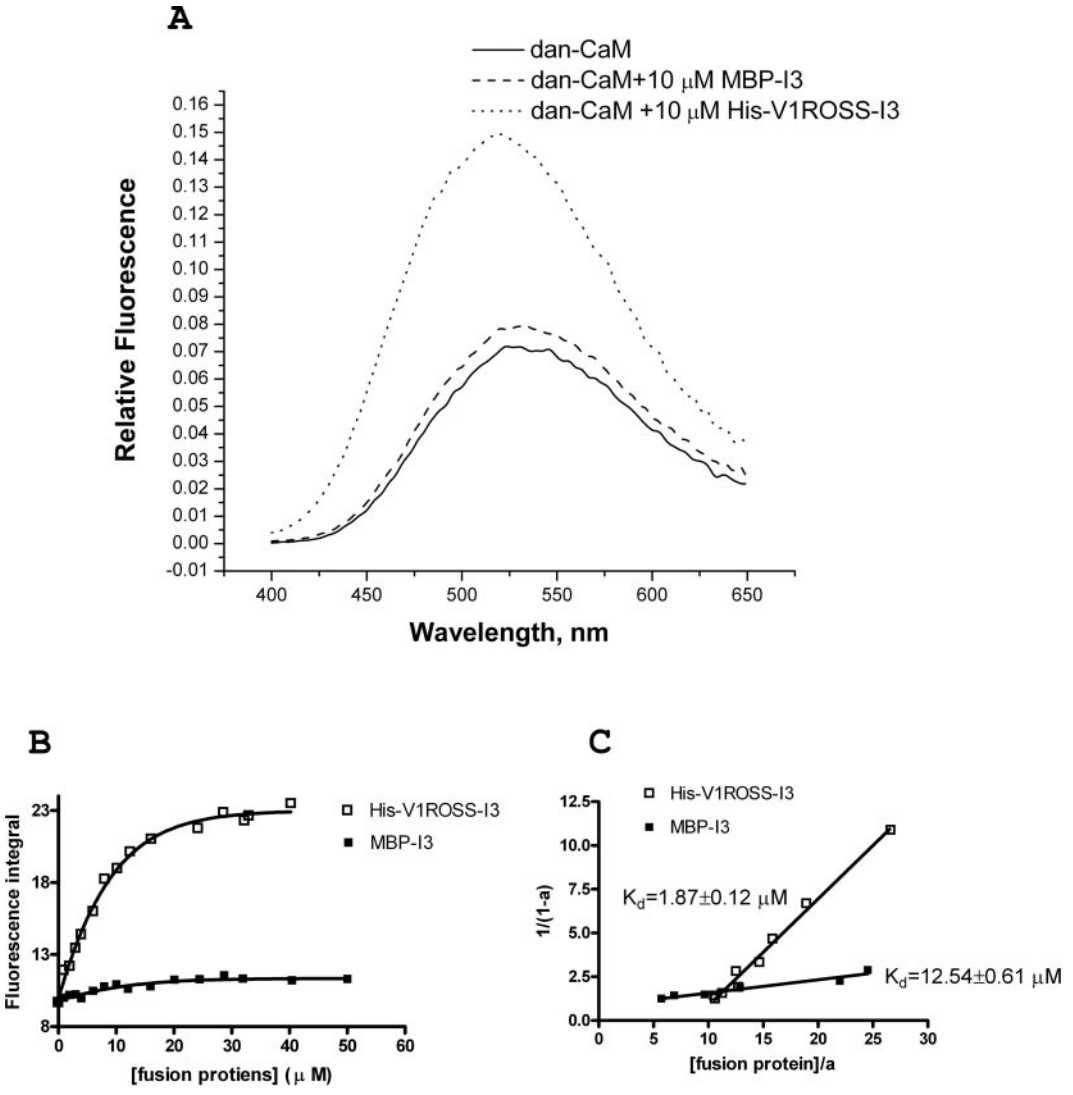

Fig. 7. Fluorescence emission spectra of dansyl calmodulin in the presence of MBP-I3 or His-V1ROSS-I3. A, addition of MBP-I3 and His-V1ROSS-I3 enhances the fluorescence emission spectrum of dansyl calmodulin. B, integrated area under the fluorescence curve is plotted against the concentration of MBP-I3 and His-V1ROSS-I3. The data were fitted to a Boltzmann sigmoidal equation. C, analysis of the data in B according to Bertrand et al. (1994). The K_d value for the interaction of calmodulin with MBP-I3 and His-V1ROSS-I3 are 12.54 $\pm$ 0.61 and 1.87 $\pm$ 0.12 μM.

soluble receptor mimics in the micromolar range should be considered substantial and meaningful. Moreover, these affinities are high enough to ensure complex formation at protein concentrations used for cocrystallization.

His-V1ROSS-I3-Ct displays higher affinity for truncated arrestin2 compared with the linear MBP fusion proteins (Table 1). This implies that the I3 and Ct moieties in the His-V1ROSS-I3-Ct protein are in a favorable spatial configuration for arrestin2 binding. Consequently, V1ROSS proteins represent better receptor analogs than peptides fused to MBP in a linear manner. This validates the concept of embedding the sequence of receptor loops in the three-dimensional structure of a scaffolding protein, in this case MBP. It is noteworthy that for full-length arrestin2 binding no advantage of V1ROSS-I3-Ct over linear MBP fusion proteins was observed. This may be a consequence of the phosphorylation requirement for tight interaction of receptor moieties with full-length arestin2. In contrast, truncated arrestin2 (1–382) binds to the receptor in a phosphorylation-independent manner (Gurevich et al., 1997; Celver et al., 2002).

Receptor analogs carrying the I3 moiety were found to bind calmodulin, a ubiquitously expressed calcium sensor protein that was shown to play an important role in various GPCR signaling pathways. Vasopressin stimulation of the hV1R leads to the mobilization of intracellular calcium, the influx of extracellular calcium, the activation of PKC and calcium/calmodulin kinase (Thibonnier et al., 2001a). Calmodulin directly interacts with several GPCRs, including metabotropic glutamate subtype 5 receptor, μ-opioid receptor, D2-dopamine receptor, 5-hydroxytryptamine 1A receptor (Turner et al., 2004), and V2 vasopressin receptor (Nickols et al., 2004). The calmodulin-binding sites on these GPCRs are located either on I3 or on Ct. Similar to arrestin2, calmodulin may compete with G proteins, but its role in signal transduction is not completely understood.

The affinity of V1ROSS-I3 for calmodulin is approximately 7-fold higher than for the linear MBP-I3 (Table 1). Thus, for the purpose of calmodulin binding V1ROSS-I3 also represents a better mimic of the third intracellular loop embedded in the hV1R than the linear MBP-I3 fusion protein.

Dansylation fluorescence was used in this work for affinity measurements. Dansyl chloride is an amine-reactive fluorescence probe that reacts with the amino terminus of proteins at close to neutral pH. In this work, the proteins were labeled at pH 7.5, suggesting that the labeling was predominantly on the N terminus of the proteins. Addition of the MBP fusion proteins changed the fluorescence emission spectrum of dansyl-arrestin2, suggesting that the interaction between these two proteins may involve the N-terminal part of arrestin2. This would be consistent with previous data indicating that β strands I, V, VI, and X of the N-terminal domain of arrestins are responsible for receptor binding (Gurevich and Benovic, 1995, 1997; Vishnivetskiy et al., 2000, 2004; Hanson and Gurevich, 2006).

In conclusion, these novel soluble hV1R receptor analogs mimic the conformation of I3 and Ct of the hV1R and their relative orientation in the intact receptor well enough to reproduce receptor interactions with at least two important signaling proteins, arrestin2 and calmodulin. Such soluble receptor analogs provide a useful tool to investigate the structure-function relationships of exposed intracellular elements of integral membrane proteins. This work sets the stage for detailed structural analysis of these biologically important protein-protein interactions.

Acknowledgments

We thank Michael Ignatov, Chia-Pin Pan, and Mary Barkley for help with the fluorescence measurements; Karen Jakes and Wesley Kroeze for consultation on DNA constructs; Cynthia Wolberger for the vector of modified MBP; and John R. Raymond and Justin H. Turner for advice on dansylation fluorescence.

References

Berrada K, Plesnicher CL, Luo X, and Thibonnier M (2000) Dynamic interaction of human vasopressin/oxytocin receptor subtypes with G protein-coupled receptor kinases and protein kinase C after agonist stimulation. *J Biol Chem* **275:**27229–27237.

Bertrand B, Wakabayashi S, Ikeda T, Pouyssegur J, and Shigekawa M (1994) The Na^+/H^+ exchanger isoform 1 (NHE1) is a novel member of the calmodulin-binding proteins. Identification and characterization of calmodulin-binding sites. *J Biol Chem* **269:**13703–13709.

Carman CV and Benovic JL (1998) G-protein-coupled receptors: turn-ons and turn-offs. *Curr Opin Neurobiol* **8:**335–344.

Celver J, Vishnivetskiy SA, Chavkin C, and Gurevich VV (2002) Conservation of the phosphate-sensitive elements in the arrestin family of proteins. *J Biol Chem* **277:**9043–9048.

Chou CL, Yip KP, Michea L, Kador K, Ferraris JD, Wade JB, and Knepper MA (2000) Regulation of aquaporin-2 trafficking by vasopressin in the renal collecting duct. Roles of ryanodine-sensitive Ca^{2+} stores and calmodulin. *J Biol Chem* **275:**36839–36846.

Datta A and Stone MJ (2003) Soluble mimics of a chemokine receptor: chemokine binding by receptor elements juxtaposed on a soluble scaffold. *Protein Sci* **12:**2482–2491.

Granier S, Terrillon S, Pascal R, Demene H, Bouvier M, Guillon G, and Mendre C (2004) A cyclic peptide mimicking the third intracellular loop of the V2 vasopressin receptor inhibits signaling through its interaction with receptor dimer and G protein. *J Biol Chem* **279:**50904–50914.

Gurevich VV and Benovic JL (1993) Visual arrestin interaction with rhodopsin: sequential multisite binding ensures strict selectivity towards light-activated phosphorylated rhodopsin. *J Biol Chem* **268:**11628–11638.

Gurevich VV and Benovic JL (1995) Visual arrestin binding to rhodopsin: diverse functional roles of positively charged residues within the phosphorylation-recognition region of arrestin. *J Biol Chem* **270:**6010–6016.

Gurevich VV and Benovic JL (1997) Mechanism of phosphorylation-recognition by visual arrestin and the transition of arrestin into a high affinity binding state. *Mol Pharmacol* **51:**161–169.

Gurevich VV and Benovic JL (2000) Arrestin: mutagenesis, expression, purification and functional characterization. *Methods Enzymol* **315:**422–437.

Gurevich EV, Benovic JL, and Gurevich VV (2004) Arrestin2 expression selectively increases during neural differentiation. *J Neurochem* **91:**1404–1416.

Gurevich VV, Dion SB, Onorato JJ, Ptasienski J, Kim CM, Sterne-Marr R, Hosey MM, and Benovic JL (1995) Arrestin interactions with G protein-coupled receptors: direct binding studies with rhodopsin, β2-adrenergic and m2 muscarinic cholinergic receptors. *J Biol Chem* **270:**720–731.

Gurevich VV and Gurevich EV (2004) The molecular acrobatics of arrestin activation. *Trends Pharmacol Sci* **25:**59–112.

Gurevich VV and Gurevich EV (2006) The structural basis of arrestin-mediated regulation of G protein-coupled receptors. *Pharmacol Ther*, in press.

Gurevich VV, Pals-Rylaarsdam R, Benovic JL, Hosey MM, and Onorato JJ (1997) Agonist-receptor-arrestin, an alternative ternary complex with high agonist affinity. *J Biol Chem* **272:**28849–28852.

Hanson SM and Gurevich VV (2006) The differential engagement of arrestin surface charges by the various functional forms of the receptor. *J Biol Chem* **281:**3458–3462.

Hoffert JD, Chou CL, Fenton RA, and Knepper MA (2005) Calmodulin is required for vasopressin-stimulated increase in cyclic AMP production in inner medullary collecting duct. *J Biol Chem* **280:**13624–13630.

Ke A and Wolberger C (2003) Insights into binding cooperativity of MATa1/MATalpha2 from the crystal structure of a MATa1 homeodomain-maltose binding protein chimera. *Protein Sci* **12:**306–312.

Krupnick JG, Gurevich VV, Schepers T, Hamm HE, and Benovic JL (1994) Arrestin-rhodopsin interaction. Multi-site binding delineated by peptide inhibition. *J Biol Chem* **269:**3226–3232.

Lefkowitz RJ and Shenoy SK (2005) Transduction of receptor signals by beta-arrestins. *Science (Wash DC)* **308:**512–517.

Li J, Edwards PC, Burghammer M, Villa C, and Schertler GF (2004) Structure of bovine rhodopsin in a trigonal crystal form. *J Mol Biol* **343:**1409–1438.

Liu J and Wess J (1996) Different single receptor domains determine the distinct G protein coupling profiles of members of the vasopressin receptor family. *J Biol Chem* **271:**8772–8778.

Mukherjee S, Palczewski K, Gurevich VV, Benovic JL, Banga JP, and Hunzicker-Dunn M (1999a) A direct role for arrestins in desensitization of luteinizing hormone/choriogonatropin receptor in porcine ovarian follicular membranes. *Proc Natl Acad Sci USA* **96:**493–498.

Mukherjee S, Palczewski K, Gurevich VV, and Hunzicker-Dunn M (1999b) β-Arrestin dependent desensitization of luteinizing hormone/choriogonadotropin receptor is prevented by a synthetic peptide corresponding to the third intracellular loop of the receptor. *J Biol Chem* **274:**12984–12989.

Nakamura K, Liu X, and Ascoli M (2000) Seven non-contiguous intracellular residues of the lutropin/choriogonadotropin receptor dictate the rate of agonist-induced internalization and its sensitivity to non-visual arrestins. *J Biol Chem* **275:**241–247.

Nickols HH, Shah VN, Chazin WJ, and Limbird LE (2004) Calmodulin interacts with the V2 vasopressin receptor: elimination of binding to the C terminus also eliminates arginine vasopressin-stimulated elevation of intracellular calcium. *J Biol Chem* **279:**46969–46980.

Okada T, Fujiyoshi Y, Silow M, Navarro J, Landau EM, and Shichida Y (2002) Functional role of internal water molecules in rhodopsin revealed by X-ray crystallography. *Proc Natl Acad Sci USA* **99:**5982–5987.

Palczewski K, Kumasaka T, Hori T, Behnke CA, Motoshima H, Fox BA, Le Trong I, Teller DC, Okada T, Stenkamp RE, et al. (2000) Crystal structure of rhodopsin: a G protein-coupled receptor. *Science (Wash DC)* **289:**739–745.

Potter RM, Key TA, Gurevich VV, Sklar LA, and Prossnitz ER (2002) Arrestin variants display differential binding characteristics for the phosphorylated *N*-formyl peptide receptor carboxyl terminus. *J Biol Chem* **277:**8970–8978.

Raman D, Osawa S, Gurevich VV, and Weiss ER (2003) The interaction with the cytoplasmic loops of rhodopsin plays a crucial role in arrestin activation and binding. *J Neurochem* **84:**1040–1050.

Rosenthal W, Antaramian A, Gilbert S, and Birnbaumer M (1993) Nephrogenic diabetes insipidus. A V2 vasopressin receptor unable to stimulate adenylyl cyclase. *J Biol Chem* **268:**13030–13033.

Thibonnier M (1998) Development and therapeutic indications of orally-active non-peptide vasopressin receptor antagonists. *Expert Opin Investig Drugs* **7:**729–740.

Thibonnier M (2003) Vasopressin receptor antagonists in heart failure. *Curr Opin Pharmacol* **3:**683–687.

Thibonnier M, Berti-Mattera LN, Dulin N, Conarty DM, and Mattera R (1998a) Signal transduction pathways of the human V1-vascular, V2-renal, V3-pituitary vasopressin and oxytocin receptors. *Prog Brain Res* **119:**147–161.

Thibonnier M, Coles P, Thibonnier A, and Shoham M (2001a) The basic and clinical pharmacology of nonpeptide vasopressin receptor antagonists. *Annu Rev Pharmacol Toxicol* **41:**175–202.

Thibonnier M, Conarty DM, Preston JA, Wilkins PL, Berti-Mattera LN, and Mattera R (1998b) Molecular pharmacology of human vasopressin receptors. *Adv Exp Med Biol* **449:**251–276.

Thibonnier M, Plesnicher CL, Berrada K, and Berti-Mattera L (2001b) Role of the human V1 vasopressin receptor COOH terminus in internalization and mitogenic signal transduction. *Am J Physiol* **281:**E81–E92.

Turner JH, Gelasco AK, and Raymond JR (2004) Calmodulin interacts with the third intracellular loop of the serotonin 5-hydroxytryptamine1A receptor at two distinct sites: putative role in receptor phosphorylation by protein kinase C. *J Biol Chem* **279:**17027–17037.

Vishnivetskiy SA, Hosey MM, Benovic JL, and Gurevich VV (2004) Mapping the arrestin-receptor interface. Structural elements responsible for receptor specificity of arrestin proteins. *J Biol Chem* **279:**1262–1268.

Vishnivetskiy SA, Schubert C, Climaco GC, Gurevich YV, Velez M-G, and Gurevich VV (2000) An additional phosphate-binding element in arrestin molecule: implications for the mechanism of arrestin activation. *J Biol Chem* **275:**41049–41057.

Address correspondence to: Dr. Menachem Shoham, Department of Biochemistry, Case Western Reserve University, 10900 Euclid Ave., Cleveland, OH 44106-4935. E-mail: mxs10@case.edu